



Effects of chronic kidney disease on cognitive function and α -klotho expression in hippocampus

Menglan Huang^{1#^}, Guangzhi Li^{2#^}, Junhua Tan^{3^}, Meiyong Huang^{3^}, Feifan Huang^{3^}, Ruiying Ma^{3^}, Yu Xiao^{3^}, Jie Wang^{3^}

¹Department of Nephrology, The People's Hospital of Baise, Baise, China; ²Department of General Medicine, Affiliated Hospital of Youjiang Medical University for Nationalities, Baise, China; ³Department of Nephrology, Affiliated Hospital of Youjiang Medical University for Nationalities, Baise, China

Contributions: (I) Conception and design: J Wang, Menglan Huang; (II) Administrative support: None; (III) Provision of study materials or patients: None; (IV) Collection and assembly of data: Menglan Huang, G Li; (V) Data analysis and interpretation: J Tan, Meiyong Huang, F Huang, R Ma, Y Xiao; (VI) Manuscript writing: All authors; (VII) Final approval of manuscript: All authors.

[#]These authors contributed equally to this work.

Correspondence to: Jie Wang. Affiliated Hospital of Youjiang Medical University for Nationalities, Zhongshan 2nd Road, No. 18 Youjiang, Baise 533000, China. Email: wangj20192022@163.com.

Background: Alpha-klotho (α -KL) is not only related to the regulation of calcium-phosphorus metabolism, and fibrosis in chronic kidney disease (CKD), it is also involved in the regulation of many cognitive disorders. We conducted this study to investigate the effects of CKD on cognitive dysfunction and α -KL.

Methods: Doxorubicin was used to induce a CKD model, which was validated by weight, 24-hour urine protein quantification, serum creatinine (Cr), blood urea nitrogen (BUN), and kidney hematoxylin-eosin (HE) staining. The Morris water maze (MWM) paradigm was used to assess the effects of CKD on cognitive behavior. The expression of α -KL in the hippocampus was detected using real-time quantitative polymerase chain reaction, Western blot, and immunohistochemistry (IHC).

Results: (I) In the CKD group, the weight of the rats increased slowly ($P < 0.001$), 24-hour urine protein increased ($P < 0.05$), and Cr ($P = 0.026$) and BUN levels ($P = 0.003$) increased; (II) HE staining showed that in the CKD group there were changes in the structure, fibrosis, and inflammatory infiltration of the renal tissues, and changes in the structure, cell necrosis, and neuronal degeneration of the hippocampus; (III) in the MWM experiment, the escape latency of the CKD group was prolonged compared to that of the control group ($P = 0.043$, 0.023), and the number of crossing the platform was reduced ($P = 0.003$); (IV) in the CKD group, the expressions of α -KL messenger ribonucleic acid ($P = 0.0005$) and α -KL protein ($P = 0.0005$) in the hippocampus were downregulated. The IHC results showed that the expression of α -KL protein in the hippocampal region III cornu ammonis (CA3) of the CKD group region was also downregulated, and the α -KL-positive cells ($P = 0.019$) and mean optical density ($P = 0.015$) were decreased.

Conclusions: The expression of α -KL appears to effect the cognitive function of CKD rats; thus, it may be a valuable target in the treatment of CKD with cognitive impairment.

Keywords: Chronic kidney disease (CKD); cognitive impairment; klotho

Submitted Jun 13, 2022. Accepted for publication Jul 29, 2022.

doi: 10.21037/tau-22-465

View this article at: <https://dx.doi.org/10.21037/tau-22-465>

[^] ORCID: Menglan Huang 0000-0001-7591-784X; Guangzhi Li, 0000-0002-3592-9931; Junhua Tan, 0000-0002-4357-9214; Meiyong Huang, 0000-0001-9744-3649; Feifan Huang, 0000-0001-9275-1159; Ruiying Ma, 0000-0002-5844-0696; Yu Xiao, 0000-0002-2504-0880; Jie Wang, 0000-0002-4479-6173.

Introduction

Chronic kidney disease (CKD) refers to a class of disorders in which the kidneys are structurally damaged and dysfunctional for >3 months (1). The global prevalence rate of CKD is 14.3% (2). We found that CKD patients are difficult to manage, show poor compliance, and have low communication efficiency, which results in a poor treatment effect and poor prognosis in practical clinical work. The key to these problems may lie in the patients' brain dysfunction. This type of cognitive impairment has the characteristics of occultity and a tendency to deteriorate, and its cause may be related to the genes, uremia toxins, blood vessels, and other factors in patients with CKD (3). Studying the mechanism of occurrence and the development of cognitive impairment caused by CKD can help solve the above-mentioned clinical problems.

Alpha-klotho (α -KL) is a type I single-passing transmembrane protein encoded by the *klotho* gene, which consists of a short cytoplasmic tail, a transmembrane domain, and two extracellular domains (K11 and K12), and is expressed primarily in the tubules, parathyroid glands, and choroid plexus (4,5). As a multifunctional pleiotropic protein, α -KL has the following 2 forms: secretory and membrane, and involves in a variety of biological and pathological functions in various organs and tissues. Kuro-o *et al.* observed that a defect in *klotho* gene expression in the mouse results in a syndrome that resembles human ageing, such as a short lifespan, infertility, arteriosclerosis, skin atrophy, cardiomyopathy, ectopic calcification, osteoporosis and emphysema (6).

Previous studies have shown that α -KL is not only involved in the regulation of calcium and phosphorus metabolism and the inhibition of renal fibrosis in CKD (7,8), but as an *in-vivo* hormone, it also exerts anti-oxidative stress, anti-inflammatory, anti-apoptotic, and autophagy-regulating effects (9-12). Under normal renal physiological conditions, α -KL, fibroblast growth factor receptor-1 (FGFR1) and fibroblast growth factor-23 (FGF23) bind to form a trimeric complex, which drives FGF23 phosphorylation and thus reduces serum Pi by inhibiting 1,25-dihydroxyvitamin D and parathyroid hormone synthesis, intestinal Pi absorption, and Pi reabsorption (13,14). In addition, α -KL has a biological function that is not dependent on FGF23. In one study of diabetic nephropathy, α -KL successfully upregulated the expression of renal transient receptor potential vanilloid type 5, which plays an important role in regulating calcium-phosphate metabolism (15).

The serum and cerebrospinal fluid levels of α -KL are positively correlated with and predict scores on the Mini-Mental State Examination and Clinical Dementia Rating, regardless of sex (16). Additionally, a study related to the most common neurodegenerative disease (i.e., Alzheimer's disease) has shown that the disease leads to decreased α -KL expression in the brain, and the overexpression of α -KL improves cognitive function by inhibiting neuroinflammation, promoting amyloid β -protein (A β) clearance, and mitigating Tau pathology (17).

Such findings suggest that α -KL is involved in the regulatory mechanisms of neurological damage. However, previous research on α -KL in CKD has mainly focused on calcium/phosphorus regulation and renal fibrosis, and research on cognition has been limited. To the studies on CKD combined with cognitive dysfunction, only a small number of studies directly or indirectly involving α -KL, because it is involved in the regulation of phosphorus and parathyroid hormone (18-20). In this study, we sought to observe the changes of α -KL in CKD rats and analyze its relationship with cognitive function to provide a theoretical basis for the further exploration of the possible mechanism of α -KL in CKD, especially in the hippocampus. We present the following article in accordance with the ARRIVE reporting checklist (available at <https://tau.amegroups.com/article/view/10.21037/tau-22-465/rc>).

Methods

Animal data and major reagents

We purchased 20, 10-week-old, male, Wistar rats from the Changsha Tianqin Biotechnology Company. The rats were maintained at a 12-hour light/dark cycle at 25 °C and about 45% relative humidity with free access to food and water. After 1 week of feeding, the rats were randomly divided into the control and CKD groups (n=10). CKD was induced by tail vein injections of doxorubicin (HY-15142, MedChem Express). In brief, the tail vein was administered at a dose of 4 mg/kg of doxorubicin on days 0 and 14 at the beginning of the experiment, respectively, and feeding then continued for 12 weeks; the control group was given an equal amount of saline. Animal experiments were performed under a project license (No. 2020060102) granted by the Ethics committee of Youjiang Medical University for Nationalities, in compliance with institutional guidelines for the care and use of animals. A protocol was prepared before the study without registration.

Table 1 Detection of the primers of the target genes by RT-qPCR

Gene name	Forward primers (5'-3')	Downstream primers (5'-3')
α -KL	CGTGAATGAGGCTCTGAAAGC	GAGCGGTCACTAAGCGAATACG
β -actin	TATCGGACGCCTGGTTAC	CTGTGCCGTTGAACTTGC

RT-qPCR, real-time quantitative polymerase chain reaction.

The following reagents were used in this study: a rat anti-Klotho [(PA5-88303), Thermo, Shanghai]; a rat anti- β -actin [(AF7018), Affinity, Shanghai]; urine protein test kit (C035-2-1), a urea assay kit (C013-2-1), and a creatinine (Cr) assay kit (C011-2-1) (Nanjing Jiancheng Corp. Nanjing, China).

MWM

In animal experiments, the Morris water maze (MWM) test is a classic experiment that is used to evaluate experimental cognitive function. At the beginning of our experiment, the vision and swimming ability of the rats in each group was assessed by an initially visible platform test. The main experiments comprise a positioning navigation test and a space exploration test, which were performed to evaluate spatial learning and memory (21). In the positioning navigation test, the rats were trained for 4 consecutive days to find the target platform that was hidden 1 cm below the surface of the water in <90 seconds each time. In the space exploration test, the rats still searched for the platform that had been removed, and the relevant parameters were recorded within 90 seconds; for example, the frequency with which the rats crossed to the location of the original platform, the total distance covered, and the time of duration in the target quadrant were recorded using the DigBehv automated tracking system (Shanghai, China).

Indicators of kidney damage

Tests for indicators of kidney damage were mainly assessed by 24-hour urine protein quantification, Cr, and blood urea nitrogen (BUN). The assays were conducted in accordance with the corresponding kit instructions.

HE staining

Tissue sections of the kidney and hippocampus were stained with hematoxylin-eosin (HE) by an automated staining machine (Leica, Germany). Rat kidneys and brains were fixed with 10% (V/V) buffered formalin for 24 h, followed

by dehydration, permeabilization, wax dipping by Leica ASP300S (a fully automatic closed tissue dewatering machine). Then, paraffin-embedded tissues were fixed and embedded in paraffin, and cutting into 3 μ m sections. The HE staining was operated automatically by a Leica fully automatic dyeing machine. The specific procedures were as follows: (I) sections were dewaxed and rehydrated, then washed, (II) immersed into Harris Haematoxylin for 5 min then washed, (III) differentiated in 3% alcohol then washed, (IV) blued in Lithium carbonate for 30 sec, then washed, (V) immersed into eosin for 1 min, then washed, (VI) dehydrated in gradient alcohol and xylene, (VII) sealed. All slides were observed and photographed under the optical microscope.

Fluorescent RT-qPCR

The specimens were ground by liquid nitrogen, and 1 mL of TRIzol was added to extract total ribonucleic acid (RNA). Next, 1 μ g of the total RNA was taken and reverse transcribed into complementary deoxyribonucleic acid (cDNA). The target sequences were amplified, and the expression levels of the target gene α -KL and housekeeping gene β -actin were quantified using the Synergy Brands (SYBR) green chimeric fluorometric method. The primer sequences used are detailed in *Table 1*. The $2^{-\Delta\Delta C_t}$ method was used to calculate the relative expression of the analyzed genes.

Western blotting

To extract the total protein, the harvested kidney and hippocampal tissues were lysed using Radio Immunoprecipitation Assay buffer (PC101, Epizyme Biomedical Technology Co., Ltd, Shanghai, China). The protein was then denatured after the protein concentration had been determined by BCA assay (BCA Protein Assay Kit; Beyotime Biotechnology Co. Ltd, China). Next, 30 μ g of protein samples were transferred to the polyvinylidene difluoride membrane by sodium dodecyl sulfate-polyacrylamide gel electrophoresis, and after blocking

at room temperature for 45 minutes with the blocking solution, the samples were incubated at 4 °C overnight with α -KL antibodies (1:400) and β -actin antibodies (1:1,000). The samples were then rinsed with tris-buffered saline and tween-20, and the secondary antibody (1:1,000) was incubated at room temperature for 1 hour, and finally the samples were then rinsed again. Immuno-blots were then incubated with ECL reagents and pictures were taken, and the relative expression of the target protein was analyzed by the Image-J Image Analysis System using β -actin as an internal reference.

IHC staining

Paraffin sections were dewaxed in water and placed in citric acid antigen repair buffer in a microwave oven for antigen repair, cooled and washed 3 times with phosphate buffered solution (PBS), and then placed in 3% hydrogen peroxide solution to block the endogenous peroxidase. Next, the tissues were blocked with 3% bovine serum albumin (BSA) in PBS for 30 minutes at room temperature. Then, the α -KL primary antibody (1:100) was incubated overnight at 4 °C. The next day, the tissues were incubated with goat anti-rabbit secondary antibodies (1:1,000) at room temperature, after rinsing three times. Finally, the sections were developed using diaminobenzidine working solution, and then counterstained with hematoxylin and sealed with neutral gum. Microscopic images were collected and analyzed by Image-Pro Plus 6.0.

Statistical analysis

The data were statistically analyzed using the SPSS 23.0 software package. The measures with a normal distribution are expressed as the mean \pm standard deviation (SD), and comparisons between the 2 groups were made using the 2 independent samples *t*-test. The measures that did not conform to a normal distribution were expressed as the median (interquartile range), and comparisons between the 2 groups were made using the Mann-Whitney U-test. A *P* value <0.05 was considered statistically significant.

Results

Doxorubicin-induced CKD model

The rats in the CKD group showed hunching, reduced eating, fur loss, reduced mobility, and periorcular and scrotal

edema after doxorubicin injection. The weight of the rats in the CKD group decreased significantly at the 6th, 10th, and 14th week compared to that of the control group ($P < 0.001$; see *Figure 1A*). Additionally, the 24-hour urine protein quantification at the end of the 2nd and 14th week ($P = 0.033$, 0.001 ; see *Figure 1B*), and the BUN ($P = 0.003$; see *Figure 1C*), and Cr ($P = 0.026$; see *Figure 1D*) levels were higher in the CKD group than the control group, and the differences were statistically significant. A total of 3 rats in the model group died during the period.

HE staining of kidney and hippocampal tissue

Under the optical microscope, the renal envelope in the control group was smooth, and the glomeruli and tubular structures were clear and intact (see *Figure 2A-2C*). Conversely, in the CKD group, the surface of the kidney was uneven, the number of tubular epithelial cells were significantly reduced, the lumen was widely dilated, a large number of protein tubular patterns was visible, and the tubules were necrotic and degenerative to different degrees. Additionally, some of the glomerular capillary collaterals were dilated, some of the glomeruli were atrophied, and a large amount of protein mucus was visible in the capsule lumen. Fibrous tissue proliferation and the focal infiltration of the inflammatory cells were clearly visible in the interstitium (see *Figure 2D-2F*).

The number of cells in the hippocampal tissue of the control group was not reduced, the pyramidal cells were arranged neatly and tightly, with a large number of layers (see *Figure 2G*), and neuronal degeneration and a small amount of cellular consolidation were occasionally seen in the region III cornus ammonis (CA3) of the hippocampus (see *Figure 2H, 2I*). Conversely, in the hippocampal tissue of the rats with CKD, the number of cells was slightly reduced, the cone cells were loosely arranged, and irregular intercellular gaps, neuronal degeneration and cellular sequestration were observed (see *Figure 2J*), especially in the CA3 area, which was not only disorganized and loosely arranged, but also accompanied by neuronal degeneration and a large amount of nuclear sequestration and cytoplasmic vacuolization (see *Figure 2K, 2L*).

MWM

In the initial visible platform test, the results of total swim distance and escape latency did not differ significantly between the 2 groups ($P = 0.522$, 0.677), suggesting that

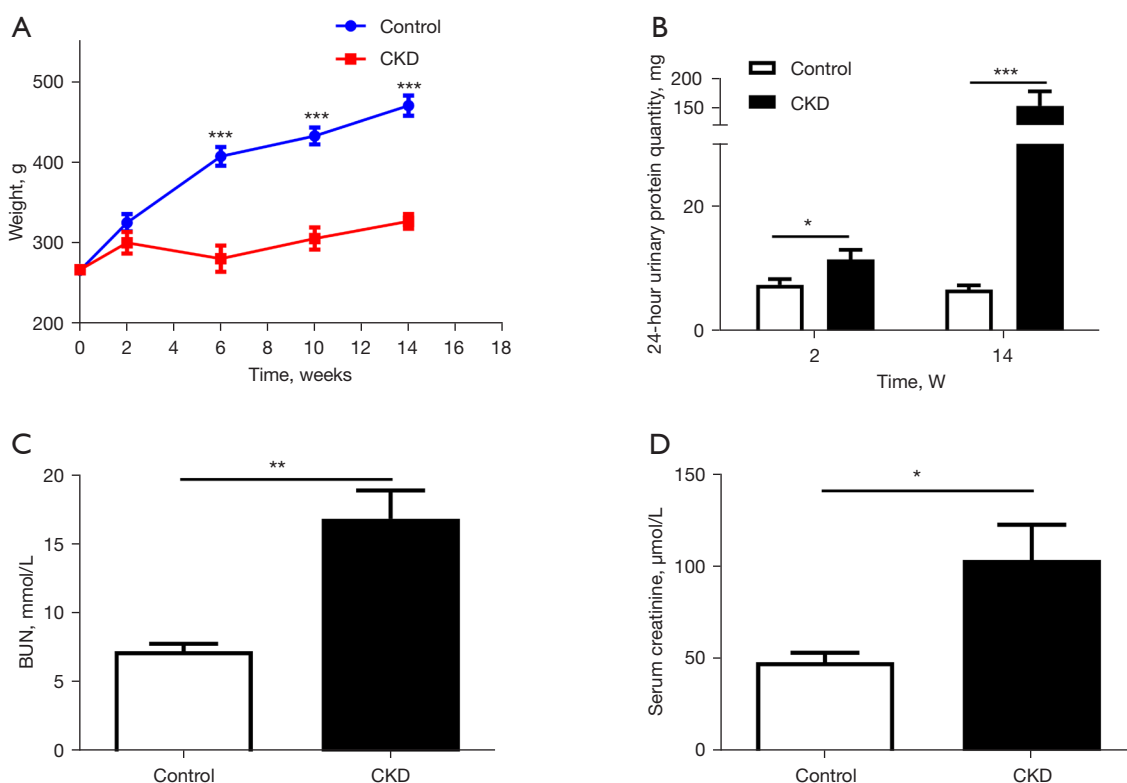


Figure 1 Validation of the doxorubicin-induced CKD model. (A) Weight changes in rats at different time points. The weight of the rats in the CKD group, at the 6th, 10th, and 14th week decreased significantly compared to that of the control group ($P < 0.001$). (B) Comparison of 24-hour urine protein quantification. The 24-hour urine protein quantification at the end of the 2nd and 14th weeks ($P < 0.05$). (C,D) Comparison of the BUN and serum Cr levels in rats. The levels of BUN (C) and serum Cr (D) were higher in the CKD group than the control group ($P < 0.05$). Ratio of CKD group to control group, * $P < 0.05$, ** $P < 0.01$, *** $P < 0.001$; control group $n = 10$, CKD group $n = 7$. CKD, chronic kidney disease; BUN, blood urea nitrogen; Cr, creatinine.

the visual acuity and swimming skills of the 2 groups were not statistically different and could be compared (see *Figure 3A, 3B*).

In the positioning navigation test, there was no statistical difference in the escape latency during the first 2 days of training; however, by the 3rd and 4th days of training, the escape latency of the CKD group was prolonged (day 3: $P = 0.043$, day 4: $P = 0.023$; see *Figure 3C*), indicating that the rats in the CKD group had impaired spatial memory for the target platform, which led to a prolongation in their search for the platform. Taking more time to find the target platform indicated impaired cognitive function in CKD rats.

In the space exploration test, compared to the control group, the number of stage crossings was reduced on both day 1 and day 2 in the CKD group rats ($P = 0.019$, 0.001 ; see *Figure 3D*). Notably, on day 2, the CKD group rats exhibited a reduction in the total swim distance, the swim

distance in target quadrant, the percentage of the swim distance in target quadrant, the time in target quadrant, and the percentage of the time in target quadrant ($P = 0.027$, 0.006 , 0.007 , 0.025 , 0.025 ; see *Figure 3E-3I*), indicating that the rats in the CKD group had impaired spatial memory for the target quadrant and target platform, which reduced the distance and time they stayed in the target quadrant. *Figure 4* shows the trajectory plots for day 1 and day 2 of the spatial exploration experiment results for both groups of rats. Together, these findings showed that the cognitive function of the rats in the CKD group was impaired.

Expression of α -KL in hippocampal tissue

The results of the western blotting analysis showed the bands of α -KL protein and β -actin (see *Figure 5A*), and the grayscale values of the strips were quantified (see *Figure 5B*).

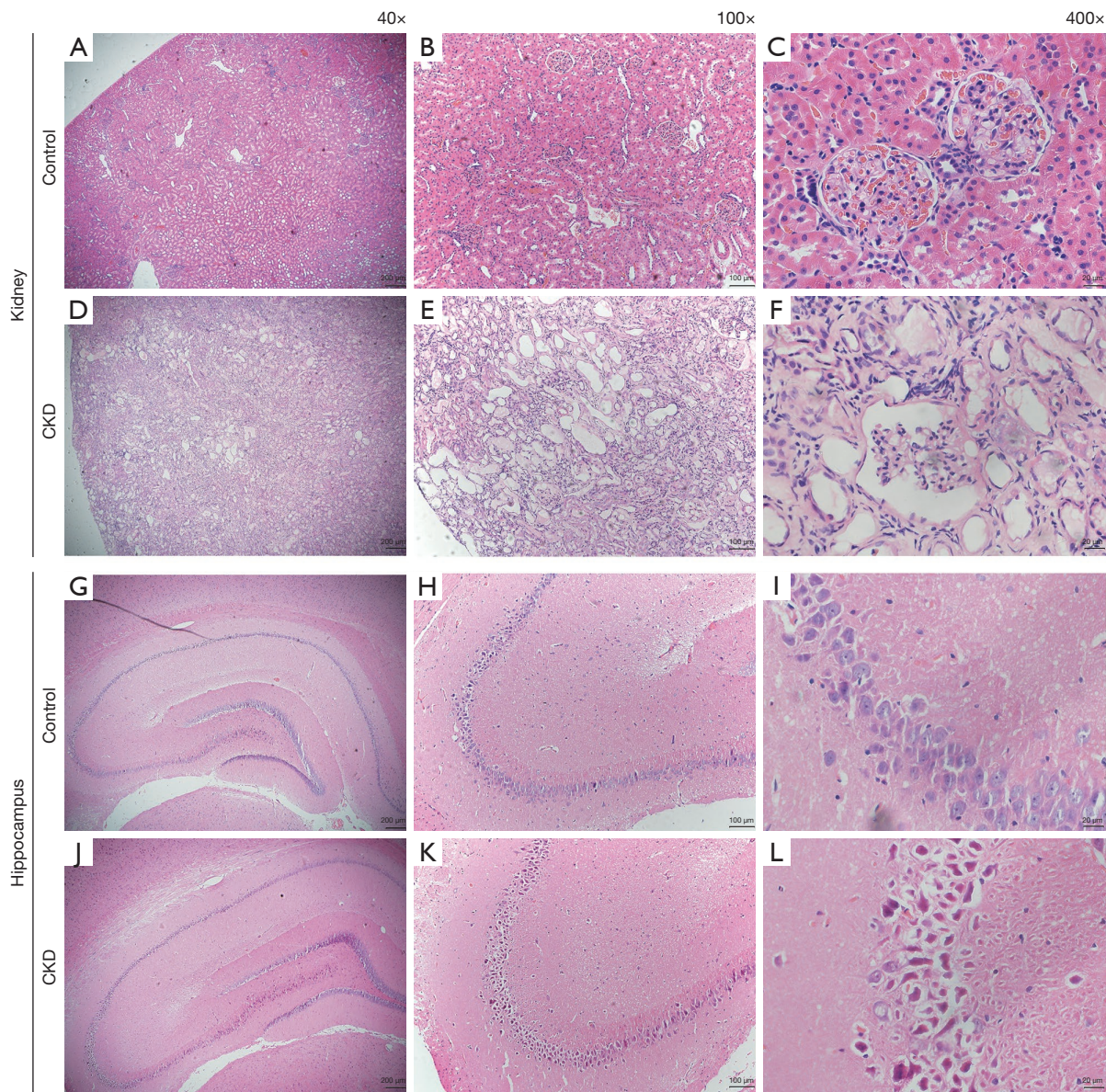


Figure 2 HE reagent staining of kidney and hippocampus. (A-C) Kidney tissue of the control group; the renal envelope in the control group was smooth, and the glomeruli and tubular structures were clear and intact. (D-F) Kidney tissue of the CKD group; the renal tissue in the CKD group showed changes in structure, fibrosis, and inflammatory infiltration. (G-I) Hippocampal tissue of the control group; no significant abnormalities in the cell morphology and structure of hippocampal tissue were observed. (J-L) Hippocampus of CKD group; hippocampal structural changes, cell necrosis, and neuronal degeneration in the CKD group were observed. (H,I,K,L) The CA3 area of the hippocampus. The images are magnified at 40, 100, and 400 times from left to right. CKD, chronic kidney disease.

The relative level of α -KL protein expression was significantly lower in the CKD group than the control group ($P=0.0005$). Similarly, the real-time quantitative polymerase chain reaction (RT-qPCR) results showed that hippocampal α -KL mRNA relative levels were significantly

lower in the CKD group than the control group ($P=0.0005$; see *Figure 5C*). The immunohistochemistry (IHC) results are shown in *Figure 5D*. *Figure 5E,5F* show the quantification of the IHC images, which showed a decrease in α -KL-positive cells ($P=0.019$) and mean optical density

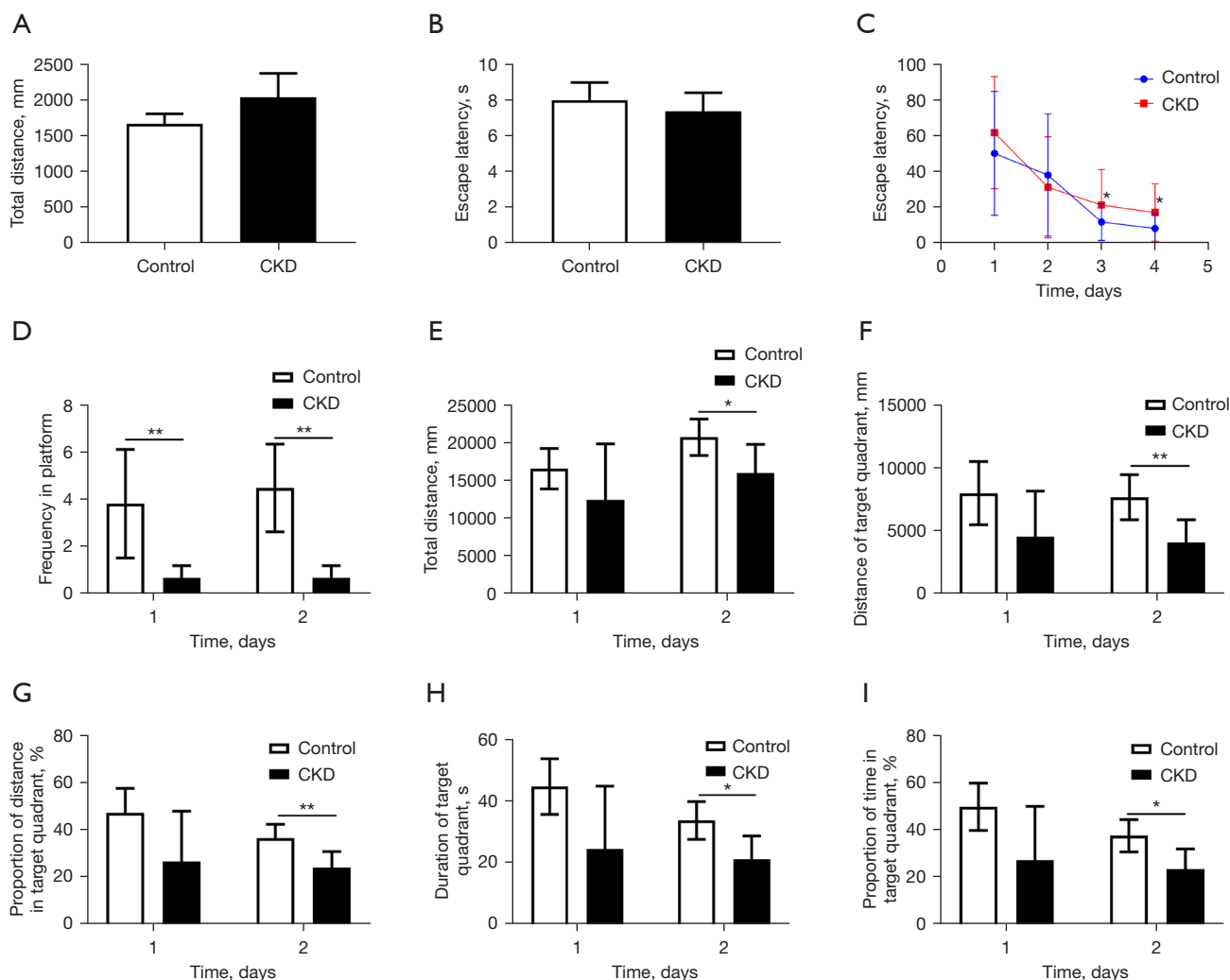


Figure 3 Behavioral experiments by Morris water maze. (A,B) Quantitative analysis of the initial visible platform test. The total distance (A) and escape latency (B) did not differ significantly between the 2 groups ($P > 0.05$). (C) The comparisons of escape latency in the positioning navigation test. After 2 days of training, the escape latency in the CKD group was longer than that of the control rats ($P < 0.05$). (D-H) The results of the space exploration test. (D) The number of crossing the platform was reduced at both day 1 and day 2 in the CKD group rats ($P < 0.01$). The CKD group rats exhibited a reduction in the total swim distance (E), the swim distance in target quadrant (F), the percentage of the swim distance in target quadrant (G), the time in target quadrant (H), and the percentage of the time in target quadrant (I) on day 2 ($P < 0.05$). * $P < 0.05$, ** $P < 0.01$; $n = 6$. CKD, chronic kidney disease.

($P = 0.015$) in the CA3 region of the hippocampus of the rats in the CKD group.

Discussion

Globally, the health burden of CKD is rapidly rising, and it has been proven to be an important independent risk factor for both cardiovascular disease and cerebrovascular disease (22). Doxorubicin can exert cytotoxic effects by

embedding DNA and inhibiting topoisomerase II, but it cannot cross the blood-brain barrier (23). Doxorubicin-induced nephrotoxic effects were found to be similar in humans and mice, with pathological manifestations characterized by inflammatory responses, apoptosis, and DNA damage (24).

In this study, a CKD model was induced in rats by 2 tail vein injections of doxorubicin. The 24-hour urine protein quantification started to increase after 2 weeks of

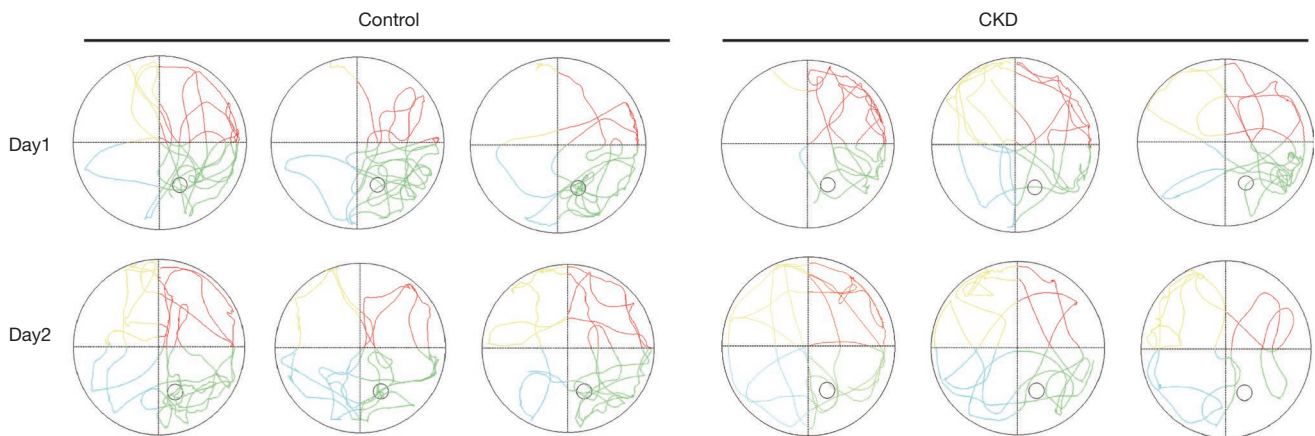


Figure 4 The trajectory diagram of the space exploration test of the Morris water maze test. The number of crossing the platform, the total swim distance, the swim distance in target quadrant, the percentage of the swim distance in target quadrant were obviously reduced in the chronic kidney disease group. CKD, chronic kidney disease.

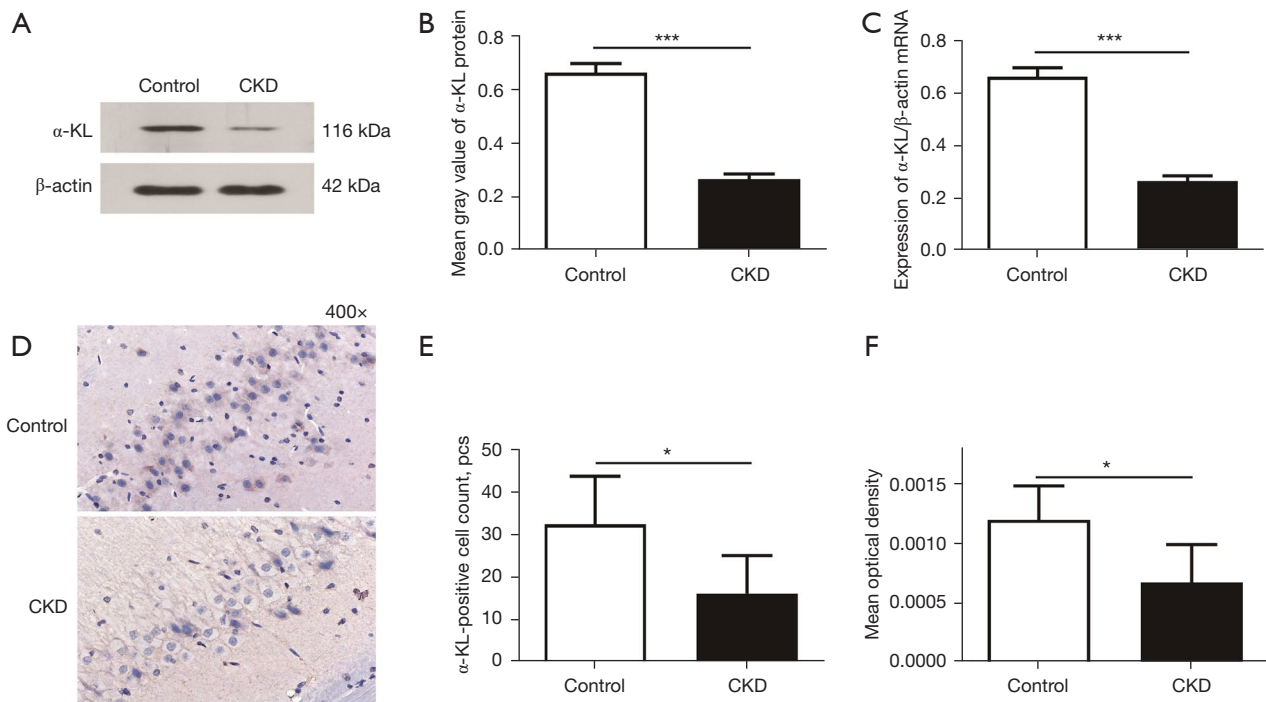


Figure 5 The expression of hippocampal α -KL was reduced in CKD rats. (A, B) The Western blotting assay revealed decreased α -KL expression in the hippocampus of the CKD rats. (C) Similarly, RT-qPCR showed that the relative expression of KL mRNA was lower in the CKD rat hippocampal tissues; internal reference: β -actin, $n=3$. (D-F) The results of IHC staining against α -KL. (D) Representative IHC images. The expression of α -KL was significantly decreased in the CA3 region of the hippocampus of the CKD rats, which was quantified as positive cell count (E) and mean optical density (F); $n=5, 7$. * $P<0.05$, *** $P<0.001$. CKD, chronic kidney disease; IHC, immunohistochemistry; RT-qPCR, real-time quantitative polymerase chain reaction.

doxorubicin injection and continued to increase for >3 months, which indicated that the doxorubicin-injected rats had persistent renal injury with a chronic course of disease development. Additionally, the Cr and BUN levels were increased, and the kidney tissue structure was obviously disordered. Further, the HE staining revealed an inflammatory reaction and fibrosis. These results all suggested that the kidney damage was clear, and that the model had been successfully established. Approximately 44% of patients with stage 3–4 CKD have combined cognitive dysfunction, and the severity of renal injury is independently and positively correlated with the severity of cognitive dysfunction, but the mechanism by which this occurs has not yet been fully elucidated (25).

Klotho is an anti-aging gene. Mice in whom the gene has been knocked out exhibit aging phenotypes, such as a short life span, atherosclerosis, skin laxity, osteoporosis, and cognitive impairment (6). α -KL also performs multiple biological functions in CKD. First, as we mentioned above, α -KL protein plays an important role in calcium and phosphorus regulation in CKD because of its involvement in the parathyroid/renal/bone axis (25). Second, α -KL not only mediated the restoration of mitochondrial function by regulating Peroxisome proliferator-activated receptor gamma coactivator 1-alpha (PGC1 α)/adenosine monophosphate-activated protein kinase (AMPK), but also inhibited the mTOR/transforming growth factor- β (TGF- β) pathway and phosphoinositide 3-kinase (PI3K)/protein kinase B (AKT)/forkhead box protein O1 (FoxO1) pathway, or activated the nuclear factor-erythroid 2-related factor 2 (Nrf2) and heme oxygenase-1 (HO-1) expression to increase antioxidant enzyme activity, scavenge reactive oxygen species, and inhibit oxidative stress and apoptosis (26–29). In addition, α -KL can inhibit the inflammatory response in CKD, exert protective effects in the cardiovascular system, as well as regulate autophagy (12,30–32). However, its role in CKD combined with cognitive dysfunction is unclear.

The hippocampus is the main site of action for memory function. A previous study showed how the hippocampus contributes to memory and cognition from different perspectives (33). α -KL is normally expressed in hippocampal cells. Xiang *et al.* injected an adeno-associated viral-mediated overexpression of *klotho* into the bilateral hippocampus of rats and found that the expression of the Nod-like receptor family pyrin domain containing 3, interleukin (IL)-1 β and caspase-1 protein were significantly alleviated, but the activation of nuclear factor erythroid 2-related factor 2 was upregulated in the brains

of the temporal lobe epilepsy model rats, which alleviated neuroinflammation, neuronal injury, and improved cognitive function (34). Additionally, α -KL was also found to have an inhibitory effect on ferroptosis in this rat model (35).

Further, some researches have shown that the overexpression of α -KL in the brain not only inhibits phosphorylation of protein kinase B (PKB or Akt) and forkhead box protein O1 (FoxO1), decreases oxidative stress, and reduces neuronal and synaptic damage, but also ameliorates neurobehavioral deficits in cerebrally under perfused mice, increases the number of live neurons in the region I cornus ammonis (CA1) and caudate shell nucleus regions of the hippocampus, and decreases nuclear translocation of nuclear factor kappa light chain enhancer of activated B cells and the production of the pro-inflammatory cytokines tumor necrosis factor alpha and IL-6 (36,37).

Additionally, α -KL is directly involved in regulating adult hippocampal neurogenesis (38). In studies on Alzheimer's disease, α -KL was found to be involved in the regulation of several mechanisms, such as microglia transformation, A β aggregation and transport, and the neuroinflammatory response (39–41). In this study, we found that the CKD rats had a longer latency period for finding the platform in the last 2 days of the positioning navigation test and a reduced number of platform crossings in the space exploration test in the MWM experiment, which suggests a decrease in their spatial memory ability. Further, α -KL mRNA, and α -KL protein were found to be more decreased in the hippocampal tissues of rats in the CKD group than the control group, which suggests that α -KL protein in hippocampal tissues is involved in the mechanism of combined cognitive impairment in CKD and leads to the downregulation of this gene expression.

The role of hippocampal area CA1 in cognition has been widely recognized. However, from the IHC staining of our hippocampal tissue, α -KL-positive cells in the CA1 region of the hippocampus were barely visible in either the control or CKD groups. It may be that α -KL mainly acts in the hippocampus in the CA3 region, but not in the CA1 region; however, this needs to be verified. In recent years, hippocampal area of CA3 has received much attention for its specific role in memory (42). The dysregulation of autophagy and apoptotic genes in the CA3 region of the hippocampus was shown to mediate cysteine-dependent neuronal death in a rat model of Alzheimer's disease (43). We assessed α -KL expression in the hippocampal tissues of rats in each group by RT-qPCR, Western blot, and IHC staining, and the results all showed decreased α -KL

expression in the hippocampus of rats with CKD, especially in the CA3 region, which suggests that the cognitive dysfunction of rats with CKD may be related to the downregulation of α -KL in hippocampal CA3.

Our study confirmed that the combined cognitive dysfunction of rats with CKD was related to the lack of α -KL in the hippocampus; however, we did not change the expression of this gene through genetic technology to explore the mechanism, which will be one of the aims of our future research. We also hope to further explore the mechanism of how α -KL affects cognitive function in CKD through cell experiments and clinical studies.

In summary, α -KL is involved in the onset and development of cognitive function in CKD rats, and its mechanism may be related to the downregulation of α -KL expression in the hippocampus. We may have revealed a novel direction for preventing or alleviating CKD-related-cognitive impairment by artificially increasing α -KL protein.

Acknowledgments

Funding: This work was supported by the Natural Science Foundation of Guangxi Province of China (No. 2019JJA140110); the High-Level Talent Research Project of The Affiliated Hospital of Youjiang Medical University for Nationalities (No. R20196341); and the Baise Scientific Research and Technology Development Program Projects (No. BS20220920).

Footnote

Reporting Checklist: The authors have completed the ARRIVE reporting checklist. Available at <https://tau.amegroupp.com/article/view/10.21037/tau-22-465/rc>

Data Sharing Statement: Available at <https://tau.amegroupp.com/article/view/10.21037/tau-22-465/dss>

Conflicts of Interest: All authors have completed the ICMJE uniform disclosure form (available at <https://tau.amegroupp.com/article/view/10.21037/tau-22-465/coif>). The authors have no conflicts of interest to declare.

Ethical Statement: The authors are accountable for all aspects of the work in ensuring that questions related to the accuracy or integrity of any part of the work are appropriately investigated and resolved. Animal

experiments were performed under a project license (No. 2020060102) granted by the Ethics committee of Youjiang Medical University for Nationalities, in compliance with institutional guidelines for the care and use of animals.

Open Access Statement: This is an Open Access article distributed in accordance with the Creative Commons Attribution-NonCommercial-NoDerivs 4.0 International License (CC BY-NC-ND 4.0), which permits the non-commercial replication and distribution of the article with the strict proviso that no changes or edits are made and the original work is properly cited (including links to both the formal publication through the relevant DOI and the license). See: <https://creativecommons.org/licenses/by-nc-nd/4.0/>.

References

- Lameire NH, Levin A, Kellum JA, et al. Harmonizing acute and chronic kidney disease definition and classification: report of a Kidney Disease: Improving Global Outcomes (KDIGO) Consensus Conference. *Kidney Int* 2021;100:516-26.
- Ene-Iordache B, Perico N, Bikbov B, et al. Chronic kidney disease and cardiovascular risk in six regions of the world (ISN-KDDC): a cross-sectional study. *Lancet Glob Health* 2016;4:e307-19.
- Viggiano D, Wagner CA, Martino G, et al. Mechanisms of cognitive dysfunction in CKD. *Nat Rev Nephrol* 2020;16:452-69.
- Erben RG, Andrukhova O. FGF23-Klotho signaling axis in the kidney. *Bone* 2017;100:62-8.
- Neyra JA, Hu MC, Moe OW. Klotho in Clinical Nephrology: Diagnostic and Therapeutic Implications. *Clin J Am Soc Nephrol* 2020;16:162-76.
- Kuro-o M, Matsumura Y, Aizawa H, et al. Mutation of the mouse klotho gene leads to a syndrome resembling ageing. *Nature* 1997;390:45-51.
- Drueke TB. Hyperparathyroidism in Chronic Kidney Disease. In: Feingold KR, Anawalt B, Boyce A et al., editors. *Endotext*. South Dartmouth (MA), 2000.
- Yuan Q, Ren Q, Li L, et al. A Klotho-derived peptide protects against kidney fibrosis by targeting TGF- β signaling. *Nat Commun* 2022;13:438.
- Li-Zhen L, Chen ZC, Wang SS, et al. Klotho deficiency causes cardiac ageing by impairing autophagic and activating apoptotic activity. *Eur J Pharmacol* 2021;911:174559.
- Zhu L, Xie H, Liu Q, et al. Klotho inhibits H2 O2

- induced oxidative stress and apoptosis in periodontal ligament stem cells by regulating UCP2 expression. *Clin Exp Pharmacol Physiol* 2021;48:1412-20.
11. Wang Y, Wang K, Bao Y, et al. The serum soluble Klotho alleviates cardiac aging and regulates M2a/M2c macrophage polarization via inhibiting TLR4/Myd88/NF- κ B pathway. *Tissue Cell* 2022;76:101812.
 12. Xue M, Yang F, Le Y, et al. Klotho protects against diabetic kidney disease via AMPK- and ERK-mediated autophagy. *Acta Diabetol* 2021;58:1413-23.
 13. Ho BB, Bergwitz C. FGF23 signalling and physiology. *J Mol Endocrinol* 2021;66:R23-32.
 14. Bacchetta J, Bardet C, Prié D. Physiology of FGF23 and overview of genetic diseases associated with renal phosphate wasting. *Metabolism* 2020;103S:153865.
 15. Lee J, Ju KD, Kim HJ, et al. Soluble α -klotho anchors TRPV5 to the distal tubular cell membrane independent of FGFR1 by binding TRPV5 and galectin-1 simultaneously. *Am J Physiol Renal Physiol* 2021;320:F559-68.
 16. Kundu P, Zimmerman B, Quinn JF, et al. Serum Levels of α -Klotho Are Correlated with Cerebrospinal Fluid Levels and Predict Measures of Cognitive Function. *J Alzheimers Dis* 2022;86:1471-81.
 17. Fung TY, Iyaswamy A, Sreenivasmurthy SG, et al. Klotho an Autophagy Stimulator as a Potential Therapeutic Target for Alzheimer's Disease: A Review. *Biomedicines* 2022;10:705.
 18. Degaspari S, Tzanno-Martins CB, Fujihara CK, et al. Altered KLOTHO and NF- κ B-TNF- α Signaling Are Correlated with Nephrectomy-Induced Cognitive Impairment in Rats. *PLoS One* 2015;10:e0125271.
 19. Li T, Xie Y, Bowe B, et al. Serum phosphorus levels and risk of incident dementia. *PLoS One* 2017;12:e0171377.
 20. Mathur A, Ahn JB, Sutton W, et al. Secondary hyperparathyroidism (CKD-MBD) treatment and the risk of dementia. *Nephrol Dial Transplant* 2022. [Epub ahead of print]. pii: gfac167. doi: 10.1093/ndt/gfac167.
 21. Trzeciakiewicz H, Ajit D, Tseng JH, et al. An HDAC6-dependent surveillance mechanism suppresses tau-mediated neurodegeneration and cognitive decline. *Nat Commun* 2020;11:5522.
 22. Kelly DM, Ademi Z, Doehner W, et al. Chronic Kidney Disease and Cerebrovascular Disease: Consensus and Guidance From a KDIGO Controversies Conference. *Stroke* 2021;52:e328-46.
 23. Ongnok B, Chattipakorn N, Chattipakorn SC. Doxorubicin and cisplatin induced cognitive impairment: The possible mechanisms and interventions. *Exp Neurol* 2020;324:113118.
 24. Bertani T, Cuttillo F, Zoja C, et al. Tubulo-interstitial lesions mediate renal damage in adriamycin glomerulopathy. *Kidney Int* 1986;30:488-96.
 25. Kuro-O M. The Klotho proteins in health and disease. *Nat Rev Nephrol* 2019;15:27-44.
 26. Lee J, Tsogbadrakh B, Yang S, et al. Klotho ameliorates diabetic nephropathy via LKB1-AMPK-PGC1 γ -mediated renal mitochondrial protection. *Biochem Biophys Res Commun* 2021;534:1040-6.
 27. Chen H, Huang X, Fu C, et al. Recombinant Klotho Protects Human Periodontal Ligament Stem Cells by Regulating Mitochondrial Function and the Antioxidant System during H₂O₂-Induced Oxidative Stress. *Oxid Med Cell Longev* 2019;2019:9261565.
 28. Xing L, Guo H, Meng S, et al. Klotho ameliorates diabetic nephropathy by activating Nrf2 signaling pathway in podocytes. *Biochem Biophys Res Commun* 2021;534:450-6.
 29. Cui W, Leng B, Wang G. Klotho protein inhibits H₂O₂-induced oxidative injury in endothelial cells via regulation of PI3K/AKT/Nrf2/HO-1 pathways. *Can J Physiol Pharmacol* 2019;97:370-6.
 30. Milovanova LY, Taranova MV, Milovanova SY, et al. Cardiovascular remodeling as a result of fibroblast growth factor-23 (FGF-23)/Klotho imbalance in patients with CKD. *Int Urol Nephrol* 2022;54:1613-21.
 31. Floege J, Fliser D. Klotho Deficiency and the Cardiomyopathy of Advanced CKD. *J Am Soc Nephrol* 2015;26:1229-31.
 32. Moreno JA, Izquierdo MC, Sanchez-Nino MD, et al. The inflammatory cytokines TWEAK and TNF α reduce renal klotho expression through NF κ B. *J Am Soc Nephrol* 2011;22:1315-25.
 33. Lisman J, Buzsáki G, Eichenbaum H, et al. Viewpoints: how the hippocampus contributes to memory, navigation and cognition. *Nat Neurosci* 2017;20:1434-47.
 34. Xiang T, Luo X, Ye L, et al. Klotho alleviates NLRP3 inflammasome-mediated neuroinflammation in a temporal lobe epilepsy rat model by activating the Nrf2 signaling pathway. *Epilepsy Behav* 2022;128:108509.
 35. Xiang T, Luo X, Zeng C, et al. Klotho ameliorated cognitive deficits in a temporal lobe epilepsy rat model by inhibiting ferroptosis. *Brain Res* 2021;1772:147668.
 36. Zhou HJ, Zeng CY, Yang TT, et al. Lentivirus-mediated klotho up-regulation improves aging-related memory deficits and oxidative stress in senescence-accelerated mouse prone-8 mice. *Life Sci* 2018;200:56-62.
 37. Zhou HJ, Li H, Shi MQ, et al. Protective Effect of Klotho

- against Ischemic Brain Injury Is Associated with Inhibition of RIG-I/NF- κ B Signaling. *Front Pharmacol* 2018;8:950.
38. Li D, Jing D, Liu Z, et al. Enhanced Expression of Secreted α -Klotho in the Hippocampus Alters Nesting Behavior and Memory Formation in Mice. *Front Cell Neurosci* 2019;13:133.
 39. Sedighi M, Baluchnejadmojarad T, Afshin-Majd S, et al. Anti-aging Klotho Protects SH-SY5Y Cells Against Amyloid β 1-42 Neurotoxicity: Involvement of Wnt1/pCREB/Nrf2/HO-1 Signaling. *J Mol Neurosci* 2021;71:19-27.
 40. Sedighi M, Baluchnejadmojarad T, Fallah S, et al. Klotho Ameliorates Cellular Inflammation via Suppression of Cytokine Release and Upregulation of miR-29a in the PBMCs of Diagnosed Alzheimer's Disease Patients. *J Mol Neurosci* 2019;69:157-65.
 41. Zhao Y, Zeng CY, Li XH, et al. Klotho overexpression improves amyloid- β clearance and cognition in the APP/PS1 mouse model of Alzheimer's disease. *Aging Cell* 2020:e13239.
 42. Cherubini E, Miles R. The CA3 region of the hippocampus: how is it? What is it for? How does it do it? *Front Cell Neurosci* 2015;9:19.
 43. Ułamek-Koziół M, Czuczwar SJ, Kocki J, et al. Dysregulation of Autophagy, Mitophagy, and Apoptosis Genes in the CA3 Region of the Hippocampus in the Ischemic Model of Alzheimer's Disease in the Rat. *J Alzheimers Dis* 2019;72:1279-86.

Cite this article as: Huang M, Li G, Tan J, Huang M, Huang F, Ma R, Xiao Y, Wang J. Effects of chronic kidney disease on cognitive function and α -klotho expression in hippocampus. *Transl Androl Urol* 2022;11(8):1157-1168. doi: 10.21037/tau-22-465